Road Adaptive Active Suspension Design Using Linear Parameter-Varying Gain-Scheduling

Ian Fialho and Gary J. Balas, *Member, IEEE*

Abstract—**This paper presents a novel approach to the design of road adaptive active suspensions via a combination of linear parameter-varying control and nonlinear backstepping techniques. Two levels of adaptation are considered: the lower level control design shapes the nonlinear characteristics of the vehicle suspension as a function road conditions, while the higher level design involves adaptive switching between these different nonlinear characteristics, based on the road conditions. A quarter car suspension model with a nonlinear dynamic model of the hydraulic actuator is employed. Suspension deflection, car body acceleration, hydraulic pressure drop, and spool valve displacement are used as feedback signals. Nonlinear simulations show that these adaptive suspension controllers provide superior passenger comfort over the whole range of road conditions.**

Index Terms—**Active suspensions, linear parameter-varying control.**

I. INTRODUCTION

ACTIVE control of vehicle suspensions has been the subject of considerable investigation since the late 1960s; see, for example, [1], [7], [8], [12], [13], [16], [18] and the references therein. Studies concerning the limitations and potential benefits of active suspensions [4], [6], [8], [9], [17] have shown that suspension controllers that focus on a fixed performance metric offer a limited improvement in performance over conventional passive suspensions, when the improvement is assessed over the whole range of road conditions. In order to realize the full potential of active suspensions the controller should have the capability of adapting to changing road environments.

Two important suspension performance metrics considered in the literature are passenger comfort and suspension deflection, i.e., the relative displacement between the car body and wheel assembly. It is widely accepted that lower vertical acceleration levels correspond to increased comfort. Structural features of a vehicle place a hard limit on the amount of suspension deflection available to reduce the car body acceleration. Hence, the goal in designing vehicle suspensions is to minimize car body acceleration, subject to the hard constraint on available suspension deflection. Typically, active suspensions are designed so that even very rough road profiles do not cause the suspension

limits to be reached; see [7] and [8]. The conservatism of this approach stems from the fact that in order to lower the vertical acceleration experienced by the car body larger suspension travel is required. Since the controller is linear, and is designed for worst-case road inputs, under normal road conditions insufficient suspension deflection is generated. As a consequence passenger comfort is lower than is possible with a nonlinear controller.

Significantly higher levels of suspension performance are achievable by designing suspension controllers that focus exclusively on minimizing car body acceleration when the suspension deflection is small, and on minimizing suspension deflection when the deflection limit is approached, thereby preventing the limit from being reached. Thus the active suspension switches from a "soft" setting to a "stiff" setting based on the magnitude of suspension deflection. Such nonlinear controllers were designed in [13] using nonlinear backstepping techniques [11], and the transition between a "soft" and "stiff" suspension was achieved by means of a novel nonlinear filter. Even higher levels of performance may be achieved by adaptively controlling the rate of transition between soft and stiff settings, based on road conditions. If the road is essentially smooth (except for the occasional large pothole, e.g., a highway), it would be preferable to maintain the soft setting for a large portion of the deflection range, rapidly switching to the stiff setting as the deflection limit is approached. Although this would result in a large vertical acceleration (due to the rapid stiffening of the suspension) as the deflection limit is approached over the rough sections, it would be a small price to pay for the superior comfort over the smooth sections. On the other hand, if the road section is essentially rough, i.e., off-road conditions, it would be preferable to start stiffening the suspension gradually over the range of suspension deflection. This road adaptive modification was discussed in reference [14].

In this paper we discuss the design of road adaptive active suspensions using linear parameter-varying (LPV) gain-scheduling [2], [3]. The LPV framework has certain advantages over the backstepping techniques used in [12]–[14]:

1) The LPV framework does not require full state-feedback, and hence only measurable signals such as suspension deflection, car body acceleration, hydraulic pressure drop, and spool valve displacement are used in the feedback loop.
2) Rapid switching between suspension settings is possible with LPV controllers. This is in contrast to reference [14], where the switching is constrained to occur only in the common zone of the different suspension settings.

I. Fialho was with the Department of Aerospace Engineering and Mechanics, University of Minnesota, Minneapolis, MN 55455 USA. He is currently with The Boeing Company, Houston, TX 77058 USA.

G. J. Balas is with the Department of Aerospace Engineering and Mechanics, University of Minnesota, Minneapolis, MN 55455 USA.

3) The LPV framework easily extends to more complex problems where steering, braking and suspensions are integrated to achieve a vehicle-level gain-scheduled control design.
4) Since LPV methods use induced norms to quantify performance, robustness (to both parametric variations and unmodeled dynamics) and sensor noise can be incorporated in the problem formulation.

We end this section with an outline of the paper. In Section II we present the nonlinear quarter car model used for suspension design, and discuss fundamental tradeoffs that motivate the design problem considered here. The design of road adaptive suspension controllers is the subject of Sections III-A and III-B. In Section III-C the controller is analyzed at fixed road condition parameter settings. Switching between the different road condition parameter settings, is discussed in Section IV. Concluding remarks are found in Section V. For the convenience of the reader, a brief discussion on linear parameter-varying methods is included in the Appendix.

II. SUSPENSION MODELING AND PERFORMANCE TRADEOFFS

The quarter car model shown in Fig. 1 will be used to design active suspension controllers. In Fig. 1 the sprung mass, m_s, represents the car chassis, while the unsprung mass, m_{us}, represents the wheel assembly. The spring, k_s, and damper, b_s, represent a passive spring and shock absorber that are placed between the car body and the wheel assembly, while the spring, k_t, serves to model the compressibility of the pneumatic tyre.

The variables x_s, x_{us}, and r are the car body travel, the wheel travel, and the road disturbance, respectively. The force f_s that is applied between the sprung and unsprung masses is generated by means of a hydraulic actuator placed between the two masses. Hence $f_s = A \cdot P_L$, where P_L is the pressure drop across the hydraulic actuator piston, and A is the piston area. The hydraulic actuator considered here is a four-way valve-piston system; see [1], [13], [15], and [16] for more details. As shown in [13] and [15] the rate of change of P_L is given by

$$\frac{V_t}{4\beta_e}\dot{P}_L = Q - C_{tp}P_L - A(\dot{x}_s - \dot{x}_{us}) \quad (1)$$

where
V_t	total actuator volume;
β_e	effective bulk modulus;
Q	load flow;
C_{tp}	total piston leakage coefficient.

The load flow is given by

$$Q = \text{sgn}[P_s - \text{sgn}(x_v)P_L]C_d w x_v \sqrt{\frac{1}{\rho}|P_s - \text{sgn}(x_v)P_L|} \quad (2)$$

where
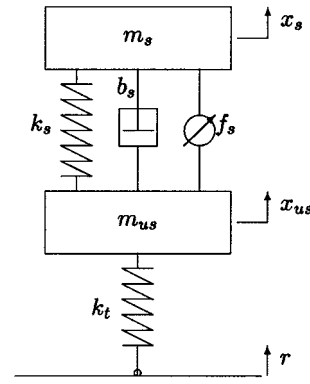|	
C_d	discharge coefficient;
w	spool valve area gradient;
x_v	displacement of the spool valve;
ρ	hydraulic fluid density;
P_s	hydraulic supply pressure.

Fig. 1. Quarter car model.

The spool valve displacement x_v is controlled by a voltage or current input u to the servovalve. The dynamics of the servovalve can be approximated as

$$\dot{x}_v = \frac{1}{\tau}(-x_v + u). \quad (3)$$

In deriving a state-space model for the quarter car dynamics it is assumed that x_s and x_{us} are measured from their static equilibrium positions and that the tyre remains in contact with the road at all times. The state variables are defined to be $x_1 := x_s$, $x_2 := \dot{x}_s$, $x_3 := x_{us}$, $x_4 := \dot{x}_{us}$, $x_5 := \mu P_L$, and $x_6 := x_v$. Observe that the pressure drop P_L has been scaled by a constant μ which was taken to be 10^{-7}, the objective of this scaling being to improve numerical conditioning during control design and closed-loop simulation. A straightforward application of Newton's law to the model shown in Fig. 1, along with the hydraulic actuator equations (1) through (3) results in the following nonlinear state-space model for the quarter car dynamics:

$$\dot{x}_1 = x_2$$
$$\dot{x}_2 = -\frac{1}{m_s}\left[k_s(x_1 - x_3) + b_s(x_2 - x_4) - \frac{A}{\mu}x_5\right]$$
$$\dot{x}_3 = x_4$$
$$\dot{x}_4 = \frac{1}{m_{us}}\left[k_s(x_1 - x_3) + b_s(x_2 - x_4)\right.$$
$$\left. -k_t(x_3 - r) - \frac{A}{\mu}x_5\right]$$
$$\dot{x}_5 = -\beta x_5 - \mu\alpha A(x_2 - x_4) + \mu\gamma x_6 w_3$$
$$\dot{x}_6 = \frac{1}{\tau}(-x_6 + u) \quad (4)$$

where

$$\alpha = \frac{4\beta_e}{V_t}, \quad \beta = \alpha C_{tp}, \quad \gamma = \alpha C_d w \sqrt{\frac{1}{\rho}}$$

and

$$w_3 = \text{sgn}\left[P_s - \text{sgn}(x_6)\frac{x_5}{\mu}\right]\sqrt{\left|P_s - \text{sgn}(x_6)\frac{x_5}{\mu}\right|}.$$

In this paper, we assume that the suspension deflection limit is ±0.08 m (8 cm), and that the maximum spool valve displace-

$m_s = 290$ kg	$\beta = 1$ sec^{-1}
$m_{us} = 59$ kg	$\gamma = 1.545 \times 10^9$ N/m$^{5/2}$kg$^{1/2}$
$b_s = 1000$ N/m/s	$\tau = 1/30$ sec
$k_s = 16812$ N/m	$P_s = 10342500$ Pa
$k_t = 190000$ N/m	$A = 3.35 \times 10^{-4}$ m^2
$\alpha = 4.515 \times 10^{13}$ N/m^5	

ment is ± 0.01 m (1 cm). The parameter values are taken from reference [13] and are listed in Table I.

Suspension Performance and Tradeoffs: In order to improve passenger comfort the transfer function $H_a(s)$ from the road disturbance r to the car body acceleration $\ddot{x}_1$ should be small in the frequency range from 0–65 rad/s. At the same time it is necessary to ensure that the transfer function $H_{sd}(s)$ from the road disturbance r to the suspension deflection $x_1 - x_3$ is small enough to ensure that even very rough road profiles do not cause the deflection limits to be reached.

The fact that the force f_s is applied between the two masses places fundamental limitations on the transfer functions $H_a(s)$ and $H_{sd}(s)$. As shown in [6], the acceleration transfer function $H_a(s)$ has a zero at the "tyrehop frequency," $\omega_1 = \sqrt{k_t/m_{us}}$. For the parameter values listed in Table I, $\omega_1 = 56.7$ rad/s. Similarly, the suspension deflection transfer function $H_{sd}(s)$ has a zero at the "rattlespace frequency," $\omega_2 = \sqrt{k_t/(m_{us} + m_s)}$. For the parameter values in Table I, $\omega_2 = 23.3$ rad/s. The tradeoff between passenger comfort and suspension deflection is captured by the fact that is not possible to simultaneously keep both the above transfer functions small around the tyrehop frequency and in the low-frequency range. In [6] it is shown that a small reduction in $H_a(s)$ at low frequencies and in the vicinity of the tyrehop frequency results in a large increase in $H_{sd}(s)$ at these frequencies and vice versa.

It follows from the previous two paragraphs that fixed linear controllers (and therefore passive suspensions) are designed to tradeoff between the conflicting tendencies of the vertical acceleration and suspension deflection transfer functions. The goal of this paper is to design suspension controllers that minimize either acceleration or suspension deflection, depending on the magnitude of suspension deflection, thereby overcoming the limitations of linear designs. When the suspension deflection is small the controller should focus on vertical acceleration, i.e., a soft setting. As the deflection limit is approached the controller should focus on preventing the suspension deflection from exceeding this limit, i.e., a stiff setting. Moreover, as discussed in the introduction, the rate of transition between the soft and stiff setting should be adaptively controlled based on the road conditions. In order to achieve these objectives, the LPV controller is designed using two scheduling parameters, ρ_{sd} and ρ_r. The parameter ρ_{sd} corresponds to suspension deflection. The parameter ρ_r is assumed to lie in the range [0, 0.1] and corresponds to the road conditions. Small values of ρ_r correspond to smooth road profiles while ρ_r values close to 0.1 correspond to rough profiles. Both these are assumed to be exogenous time-varying

parameters during the design stage. The LPV controller is designed so that when ρ_r is small (smooth roads) the controller focuses on minimizing acceleration for a range of ρ_{sd} values around zero and rapidly switches focus to minimizing suspension deflection as ρ_{sd} approaches the deflection limit of 0.08 m. When ρ_r is large (rough roads) the controller gradually switches focus from acceleration to deflection as ρ_{sd} varies from zero to 0.08 m. Since the LPV controller guarantees stability and performance over bounded ρ_{sd}, ρ_r trajectories, during controller implementation we can set ρ_{sd} to be equal to the current suspension deflection (or a magnitude limited version thereof) and ρ_r to be equal to a bounded and continuous signal that quantifies road conditions; see Remark 1 for a discussion. This results in a controller that achieves the desired objectives.

III. ROAD ADAPTIVE SUSPENSION DESIGN

This section presents the design of a road adaptive suspension controller that achieves the objectives discussed in the preceding sections. The controller uses measurements of suspension deflection ($x_1 - x_3$), piston pressure drop (x_5), car body acceleration ($\ddot{x}_1$) and spool valve displacement (x_6), and schedules on two parameters, ρ_{sd} and ρ_r, which correspond to suspension deflection and road conditions, respectively. In order to compensate for the nonlinear dynamics of the hydraulic actuator we divide the control design into two steps.

Step 1) (LPV Design)

In this step we design an LPV controller that schedules on $\rho = [\rho_{sd}, \rho_r]$, and achieves the response characteristics outlined in the previous section. The nonlinear load flow term $x_6 w_3$ in the suspension model (4) is treated as a fictitious control variable $\tilde{u}$, resulting in the following state-space model that is used for the LPV design:

$$\dot{x}_1 = x_2,$$
$$\dot{x}_2 = -\frac{1}{m_s}\left[k_s(x_1 - x_3) + b_s(x_2 - x_4) - \frac{A}{\mu}x_5\right]$$
$$\dot{x}_3 = x_4$$
$$\dot{x}_4 = \frac{1}{m_{us}}\left[k_s(x_1 - x_3) + b_s(x_2 - x_4)\right.$$
$$\left. - k_t(x_3 - r) - \frac{A}{\mu}x_5\right]$$
$$\dot{x}_5 = -\beta x_5 - \mu\alpha A(x_2 - x_4) + \mu\gamma\tilde{u}. \quad (5)$$

Step 2) (Compensating for the hydraulic actuator nonlinearity)

In this step we use nonlinear backstepping techniques [11] to choose the servovalve voltage, u, such that the nonlinear term $x_6 w_3$ is close to the fictitious control signal $\tilde{u}$.

A. LPV Controller Design

The interconnection used to design the LPV part of the suspension controller is shown in Fig. 2.

The LPV controller uses measurements of the suspension deflection ($y_1 = x_1 - x_3$), piston pressure drop ($y_2 = x_5$), and
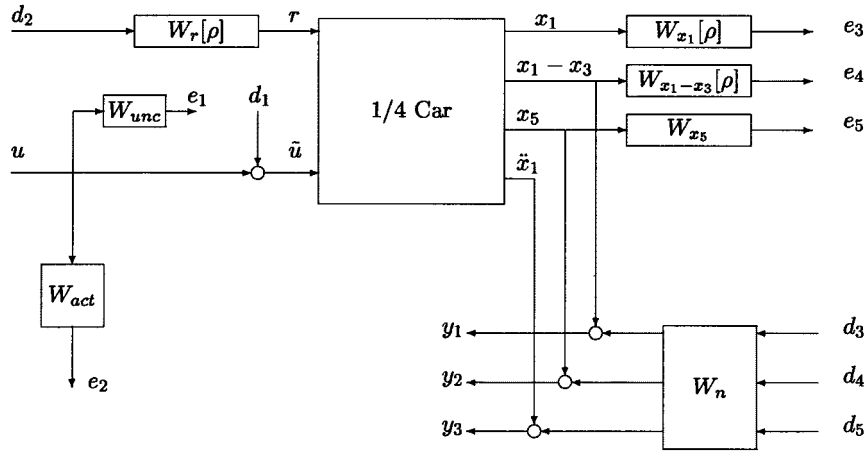
Fig. 2. LPV control design interconnection.

car body acceleration ($y_3 = \ddot{x}_1$), and schedules on the parameter $\rho = [\rho_{sd}, \rho_r]$. As in standard $\mathcal{H}_\infty$ design, the performance objectives are achieved by using frequency dependent weighting functions to penalize the signals of interests. The difference in the LPV design is that to achieve a shift in focus from vertical acceleration to suspension deflection the weights associated with some of the signals are allowed to be dependent on the scheduling parameter ρ as well. The main parameter-dependent weighting functions in Fig. 2 are $W_{x_1}[\rho]$ and $W_{x_1-x_3}[\rho]$. The weight $W_{x_1}[\rho]$ is used to penalize the vertical acceleration,[1] while $W_{x_1-x_3}[\rho]$ penalizes suspension deflection. We vary the gain of these weights, as a function of the scheduling parameter ρ, to capture the relative importance of vertical acceleration and deflection at the different parameter values. Denoting the parameter-dependent gains by $\phi_a[\rho_{sd}, \rho_r]$ and $\phi_d[\rho_{sd}, \rho_r]$, we choose $W_{x_1}[\rho]$ to have the realization

$$\dot{x} = -2\pi 10 x + \sqrt{2\pi 10 \phi_a[\rho_{sd}, \rho_r]}\, u$$
$$y = \sqrt{2\pi 10 \phi_a[\rho_{sd}, \rho_r]}\, x \tag{6}$$

and $W_{x_1-x_3}[\rho]$ to have the realization

$$\dot{x} = -10 x + \sqrt{10 \phi_d[\rho_{sd}, \rho_r]}\, u.$$
$$y = \sqrt{10 \phi_d[\rho_{sd}, \rho_r]}\, x. \tag{7}$$

Notice that at a fixed parameter value $W_{x_1}[\rho]$ is simply a first-order linear time-invariant weight with transfer function

$$\frac{2\pi 10 \cdot \phi_a[\rho_{sd}, \rho_r]}{s + 2\pi 10}.$$

Similarly, at a fixed parameter value $W_{x_1-x_3}[\rho]$ is a linear time-invariant weight with transfer function

$$\frac{10 \cdot \phi_d[\rho_{sd}, \rho_r]}{s + 10}.$$

Thus the pole locations of the weights are constant, while the gain is allowed to vary as a function of parameter values. For a fixed ρ value, the weight $W_{x_1}[\rho]$ begins rolling off before the tyrehop zero at $\omega_1 = 56.7$ rad/s. This is done to respect the well-known $\mathcal{H}_\infty$ design rule-of-thumb that requires the performance weights to roll off before an open-loop zero. We do not

roll the weight back up after the zero since we are only interested in acceleration performance in the 0–65 rad/s frequency range. In any case, as shown in reference [17], $H_a(s) = O(s^{-2})$ [i.e., $s^2 H_a(s)$ tends to a finite, possibly zero, limit as $s \to \infty$], and hence penalizing acceleration at higher frequencies offers no significant benefit. Similar reasoning is used to explain the roll-off of the weight $W_{x_1-x_3}[\rho]$ before the rattlespace zero at $\omega_2 = 23.3$ rad/s.

To capture the desired suspension response characteristics, for small values of ρ_r (smooth roads) $\phi_a[\cdot]$ (respectively, $\phi_d[\cdot]$) should be large (respectively, small) for a significant part of the ρ_{sd} range, and then rapidly become small (respectively, large) as the ρ_{sd} limit approaches. On the other hand, for large values of ρ_r (rough roads) $\phi_a[\cdot]$ (respectively, $\phi_d[\cdot]$) should gradually change from a large (respectively, small) value to a small (respectively, large) value as ρ_{sd} varies from zero to the deflection limit. Plots of the parameter-dependent gains $\phi_a[\cdot]$ and $\phi_d[\cdot]$ versus ρ_{sd}, for fixed values of ρ_r are displayed in Fig. 3.

Observe that the maximum value of $\phi_d[.]$ (as a function of ρ_{sd}) is larger for smaller values of ρ_r. The reason for this is that when ρ_r is small, the controller stiffens rapidly as the deflection limit is approached and hence should focus very strongly of deflection during the stiffening. On the other hand, when ρ_r is large the controller stiffens very gradually and hence can be less aggressive in limiting suspension deflection. Expressions for $\phi_a[\cdot]$ and $\phi_d[\cdot]$ are as follows:

$$\phi_a[\rho_{sd}, \rho_r]$$
$$= 25 \quad \text{if} \quad |\rho_{sd}| < \rho_1[\rho_r]$$
$$= \frac{25}{\rho_1[\rho_r] - 0.08}[|\rho_{sd}| - 0.08] \quad \text{if} \quad \rho_1[\rho_r] \le |\rho_{sd}| \le 0.08$$
$$= 0 \quad \text{otherwise}$$

and

$$\phi_d[\rho_{sd}, \rho_r]$$
$$= 0 \quad \text{if} \quad |\rho_{sd}| < \rho_1[\rho_r]$$
$$= \frac{\phi[\rho_r]}{0.08 - \rho_1[\rho_r]}[|\rho_{sd}| - \rho_1[\rho_r]] \text{ if } \rho_1[\rho_r] \le |\rho_{sd}| \le 0.08$$
$$= \phi[\rho_r] \quad \text{otherwise}$$

---

[1]$W_{x_1}[\rho]$ penalizes car body travel x_1 instead of $\ddot{x}_1$. These, however, are equivalent since $\ddot{X}_1(s) = s^2 X_1(s)$.
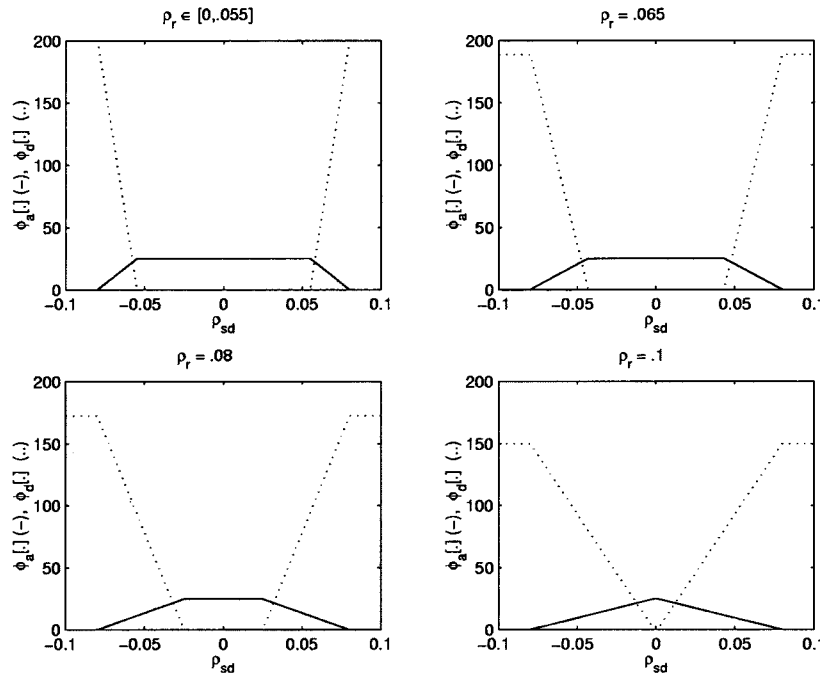
Fig. 3. $\phi_a[\cdot]$ (solid) and $\phi_d[\cdot]$ (dot) versus ρ_{sd} for various ρ_r values.

where the function $\rho_1[\rho_r]$ that determines the rate of transition between the "soft" and "stiff" setting as a function of ρ_r, and the function $\phi[\rho_r]$ that allows us to vary the maximum value of $\phi_d[.]$ (as a function of ρ_{sd}) are defined as

$$\rho_1[\rho_r] = 0.055 \quad \text{if} \quad \rho_r < 0.055$$
$$= 0.001 + \frac{0.055 - 0.001}{0.055 - 0.1}[\rho_r - 0.1] \text{ if } .055 \le \rho_r \le 0.1$$

and

$$\phi[\rho_r] = 200 \quad \text{if} \quad \rho_r < 0.055$$
$$= 150 + \frac{200 - 150}{0.055 - 0.1}[\rho_r - 0.1] \quad \text{if} \quad .055 \le \rho_r \le 0.1.$$

We now proceed to discuss the remaining weighting functions used in the LPV control design interconnection of Fig. 2.

Uncertainty and Noise Weights: The weight W_{unc} is used to incorporate robustness to unmodeled dynamics into the control design, and captures a level of unstructured multiplicative uncertainty at the plant input. It is chosen to be

$$W_{unc} = \frac{(s + 2\pi 10)}{s + 2\pi 1000}.$$

This choice corresponds to a negligible uncertainty level below 10 Hz, and 100% uncertainty at high frequency. The weight W_n is used to model sensor noise. This is chosen to be a 3×3 diagonal matrix given by $W_n = \text{diag}[0.001, 0.01, 0.01]$.

Actuator Weights: The weight W_{x_5} is used to penalize the piston pressure drop x_5. Its purpose is to limit high pressure transients that could potentially generate noise or cause excessive stress levels in the hydraulic components. We choose $W_{x_5} = 1/2$. Recall that $x_5 = 10^{-7}P_L$ and that the

supply pressure P_s is approximately 10^7 Pa. Hence, this choice corresponds to limiting the piston pressure to be no more than twice the supply pressure P_s. The weight W_{act} is used to limit the fictitious control signal $\tilde{u} = w_3 x_6$, which physically corresponds to the load flow through the spool valve. The maximum of the term $w_3 x_6$ over a pressure range of $\pm 2P_s$ and the spool valve displacement range of ± 0.01 m is 44.7214. Therefore W_{act} is chosen to be constant weight, $W_{act} = 1/50$, in order to limit $w_3 x_6$ to this maximum value.

Reference Weights: The reference weight W_r is used to shape the magnitude and frequency content of the road disturbance signal r. This was chosen to be parameter-dependent with a realization

$$\dot{x} = -2\pi 10 x + \sqrt{2\pi 10 \phi_r[\rho_{sd}, \rho_r]}\, u$$
$$y = \sqrt{2\pi 10 \phi_r[\rho_{sd}, \rho_r]}\, x.$$

Observe that at a fixed parameter value W_r is simply a linear time-invariant weight with transfer function

$$\frac{2\pi 10 \phi_r[\rho_{sd}, \rho_r]}{s + 2\pi 10}.$$

Thus the pole location is constant while the gain varies as a function of the parameter value. The weight rolls off above 10 Hz to reflect the fact that high-frequency deviations in the road surface have significantly lower amplitude compared to low-frequency deviations (see [5]). Fig. 4 shows the variation of the gain $\phi_r[\rho_{sd}, \rho_r]$ as a function of parameter values.

For $\rho_r \in [0, 0.055]$, $\phi_r[.]$ is small for a significant part of the ρ_{sd} range and then increases at larger ρ_{sd} values. This reflects the fact that points corresponding to smaller ρ_{sd} values should be optimized with respect to lower levels of road disturbance. At
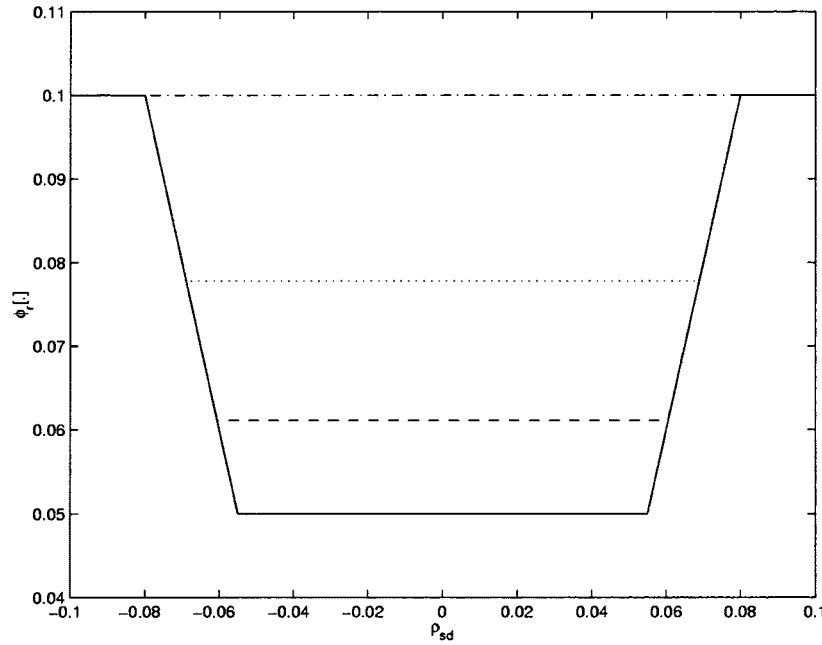
Fig. 4. $\phi_r[.]$ versus ρ_{sd} for $\rho_r \in [0, 0.055]$ (solid), 0.065 (dash), 0.08 (dot) and 0.1 (dash dot).

higher ρ_r values $\phi_r[.]$ is chosen to be larger since points corresponding to higher ρ_r values should be optimized with respect to higher levels of road disturbances. The explicit expression for $\phi_r[.]$ is similar to those for $W_{x_1}[\rho]$ and $W_{x_1-x_3}[\rho]$, and hence we do not display it here.

Remark 1: It is important to note that the car model used in the control design interconnection of Fig. 2 is linear and time-invariant, and hence the parameter-varying nature of the interconnection is due solely to the parameter-dependent weights $W_{x_1}[\rho]$, $W_{x_1-x_3}[\rho]$ and $W_r[\rho]$. The actual implemented closed-loop system will be of the form $[P, K[\rho]]$. The LPV design assures us that the closed loop will be exponentially stable for any ρ trajectory that takes values in a closed and bounded set and has at most a finite number of discontinuities in any interval; see the Appendix for the LPV problem formulation. We can always guarantee that ρ_{sd} is bounded by choosing $\rho_{sd}(t) = \mathrm{sat}(x_1(t) - x_3(t))$ if necessary, where the saturation limits can be chosen to be the bounds of the parameter variation set used in the LPV design. If $|x_1 - x_3|$ exceeds this limit the scheduling variable input to the LPV controller will be held at this limit, and hence the controller dynamics will be held at that corresponding to the saturation bounds until $|x_1 - x_3|$ falls below the saturation limit again. By design, the LPV closed-loop system is stable in this duration, and hence $|x_1 - x_3|$ cannot grow without bound. The "finite number of discontinuities condition" is always met for ρ_{sd} since physical motion must be continuous. The road condition scheduling variable ρ_r is bounded by definition. We can ensure that it is continuous by passing it through a filter before it enters the LPV controller. □

1) LPV Controller Synthesis: The synthesis of an LPV controller for the control design interconnection of Fig. 2 involves solving a set of affine matrix inequalities (AMIs); see [2] for details. The AMIs represent an infinite number of constraints since the inequalities must hold for every parameter value. For com-

putational purposes, these are approximated by a finite number of constraints by gridding the parameter space. As a consequence, the LPV controller that results is defined only at the grid points. Typically, linear interpolation between these grid points is used to define the scheduled controller as a continuous function of the parameter values. In the present design we choose the following $[\rho_{sd}, \rho_r]$ grid:

$$\rho_{sd} = [-0.1, -0.08, -0.065, -0.055, -0.025, -0.001, 0$$
$$0.001, 0.025, 0.055, 0.065, 0.08, 0.1]$$
$$\rho_r = [0\, 0.055\, 0.1].$$

It follows from the definition of the parameter-dependent weights that the 39 grid points actually correspond to only ten distinct control design interconnections. Hence only ten different $[A_K, B_K, C_K, D_K]$ matrix quadruples need to be stored in order to implement the LPV controller.

We denote the control design interconnection of Fig. 2 by $P[\rho]$. For $P[\rho]$ "frozen" at a fixed parameter value ρ, let $\gamma_{hinf}(\rho)$ be the achievable $\mathcal{H}_\infty$ performance over fixed, linear controllers. The outputs of the parameter-dependent interconnection of Fig. 2 are scaled by the parameter-dependent matrix

$$W[\rho] = \mathrm{diag}\left(\frac{1}{\gamma_{hinf}(\rho)}, \frac{1}{\gamma_{hinf}(\rho)}, \frac{1}{\gamma_{hinf}(\rho)}, \right.$$
$$\left. \frac{1}{\gamma_{hinf}(\rho)}, \frac{1}{\gamma_{hinf}(\rho)}, 1, 1, 1\right)$$

prior to performing the controller synthesis. This scaling normalizes the achievable $\mathcal{H}_\infty$ performance across the parameter set to one. The goal is to prevent any single plant $P[\rho]$ from "dominating" in the LPV design.

B. Compensating for the Hydraulic Actuator Nonlinearity

We now discuss the application of a single nonlinear backstepping step to compensate for the hydraulic nonlinearity $w_3 x_6$. Define the error variable

$$z = x_6 w_3 - \tilde{u}$$

where $\tilde{u}$ is the output of the LPV controller designed in Section III-A. If z is small then $x_6 w_3$ is close to the desired value $\tilde{u}$. Now

$$\dot{z} = \frac{d}{dt}(x_6 w_3) - \dot{\tilde{u}}$$
$$= \frac{1}{\tau}[-x_6 + u]w_3 - \frac{1}{2|w_3|}|x_6|w_2 - \dot{\tilde{u}}$$

where

$$w_2 = \frac{\dot{x}_5}{\mu} := -\frac{\beta}{\mu}x_5 - \alpha A(x_2 - x_4) + \gamma x_6 w_3.$$

Note that from (4)

$$x_2 - x_4 = \frac{1}{b_s}\left[\frac{A}{\mu}x_5 - k_s(x_1 - x_3) - m_s \ddot{x}_1\right]$$

and hence w_2 is a function of measured signals alone. If we set the servovalve voltage to be

$$u = \frac{\tau}{w_3}\left[\frac{x_6 w_3}{\tau} + \frac{1}{2|w_3|}|x_6|w_2 + \dot{\tilde{u}} - c_1 z\right] \qquad (8)$$

then the $\dot{z}$ equation becomes

$$\dot{z} = -c_1 z.$$

The closed-loop equations (in the new coordinates) are

$$\dot{x}_1 = x_2,$$
$$\dot{x}_2 = -\frac{1}{m_s}\left[k_s(x_1 - x_3) + b_s(x_2 - x_4) - \frac{A}{\mu}x_5\right]$$
$$\dot{x}_3 = x_4$$
$$\dot{x}_4 = \frac{1}{m_{us}}\left[k_s(x_1 - x_3) + b_s(x_2 - x_4)\right.$$
$$\left. -k_t(x_3 - r) - \frac{A}{\mu}x_5\right]$$
$$\dot{x}_5 = -\beta x_5 - \mu\alpha A(x_2 - x_4) + \mu\gamma\tilde{u} + \mu\gamma z$$
$$\dot{z} = -c_1 z. \qquad (9)$$

Defining $\overline{x}$ to be the combination of the states $x_1, \ldots, x_5$ and the state x_K of the LPV controller, (9) can be written more concisely as

$$\dot{\overline{x}} = f(\overline{x}, \rho, r, z) \qquad (10)$$
$$\dot{z} = -c_1 z. \qquad (11)$$

It follows from the fact that the LPV controller globally exponentially stabilizes the system (5) that $\overline{x} = 0$ is a globally

exponentially stable equilibrium point for the subsystem $\dot{\overline{x}} = f(\overline{x}, \rho, 0, 0)$ and that this subsystem has finite gain from (r, z) to $\overline{x}$. Therefore if $c_1 > 0$, the closed-loop system appears as the cascade of an exponentially stable first-order linear time-invariant system (z subsystem) and a globally exponentially stable, finite-gain subsystem [the system in (10)]. Hence the closed-loop system is stable and $\overline{x}$ and z remain bounded in response to bounded road disturbances. This is true for any positive value of c_1, however small values may result in large errors. In our simulations we set $c_1 = 100$. Since w_3 appears in the denominator of the control (8), in order to avoid division by zero we use the modification proposed in [12]:

$$\text{Set } w_3 = 1 \text{ if } 0 \leq w_3 \leq 1$$

and

$$\text{Set } w_3 = -1 \text{ if } -1 \leq w_3 < 0$$

in the denominator of (8).

Remark 2: The controller defined in (8) requires computation of the rate-of-change of $\tilde{u}$, i.e., the output of the LPV controller. In our case, it turns out that the LPV controller has a zero direct feedthrough term, i.e., has a realization of the form

$$\dot{x}_K = A_K(\rho)x_K + B_K(\rho)y$$
$$\tilde{u} = C_K(\rho)x_K.$$

It is clear that discontinuous jumps in the parameter ρ would lead to the derivative operator being ill defined. This can be overcome by filtering out any high-frequency variations in ρ before feeding it into the LPV controller. It follows from Remark 1 that this filtering does not compromise stability of the closed loop. It does, however, lead to a controller that reacts slower to variations in the scheduling variables. $\qquad \square$

C. Controller Analysis

The LPV controller designed in Section III-A has nine states, and is implemented by linearly interpolating between the controller $[A_K, B_K, C_K, D_K]$ matrices at the parameter grid points. We consider the frequency response plots of the closed-loop system obtained by interconnecting the system in (5) with the LPV controller frozen at representative grid parameter values. These are displayed in Fig. 5.

For comparison, the frequency response of the passive suspension is shown by the solid plots. Our choice of parameter-dependent weighting functions dictate that at $\rho = [0, 0]$ the controller should focus exclusively on minimizing acceleration. This is shown by the dash-dot frequency response plots in Fig. 5. When $\rho = [0.08, 0]$ the controller should focus exclusively on minimizing suspension deflection. This is shown by the dashed plots in Fig. 5. Similarly at $\rho = [0.055, 0.1]$ the controller should focus on a combination of acceleration and deflection, while at $\rho = [0.08, 0.1]$ the controller should focus on suspension deflection. This is shown by the dotted and point type responses, respectively. From Fig. 5 we see that the LPV controller shifts focus from minimizing acceleration to minimizing deflection, in a manner consistent with our choice of parameter-dependent weighting functions.
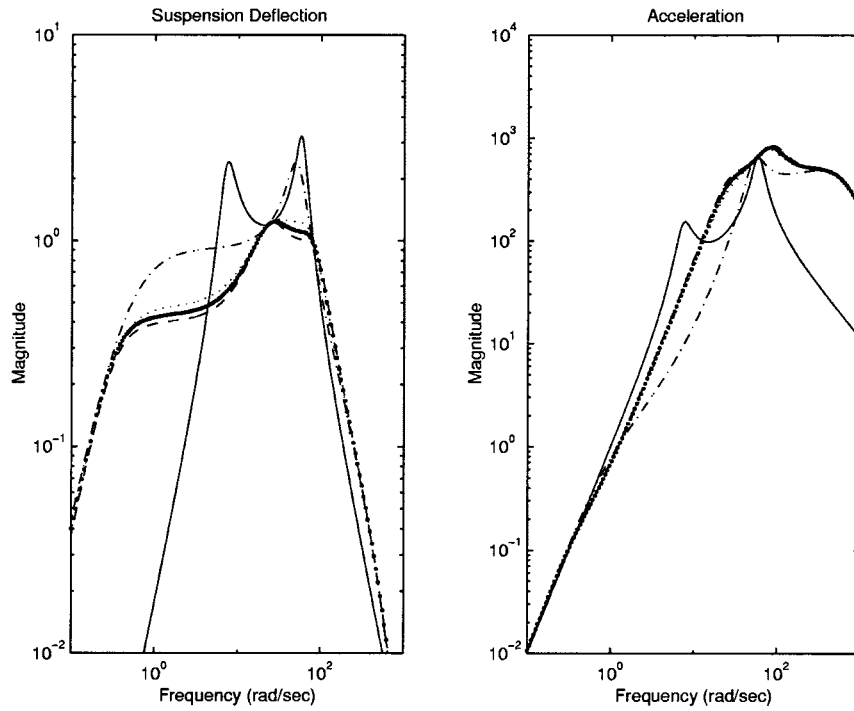
Fig. 5.   LPV controller: "frozen" closed-loop frequency responses, $\rho = [0, 0]$ (dash dot), $\rho = [0.08, 0]$ (dash), $\rho = [0.055, 0.1]$ (dot), $\rho = [0.08, 0.1]$ (point), passive (solid).
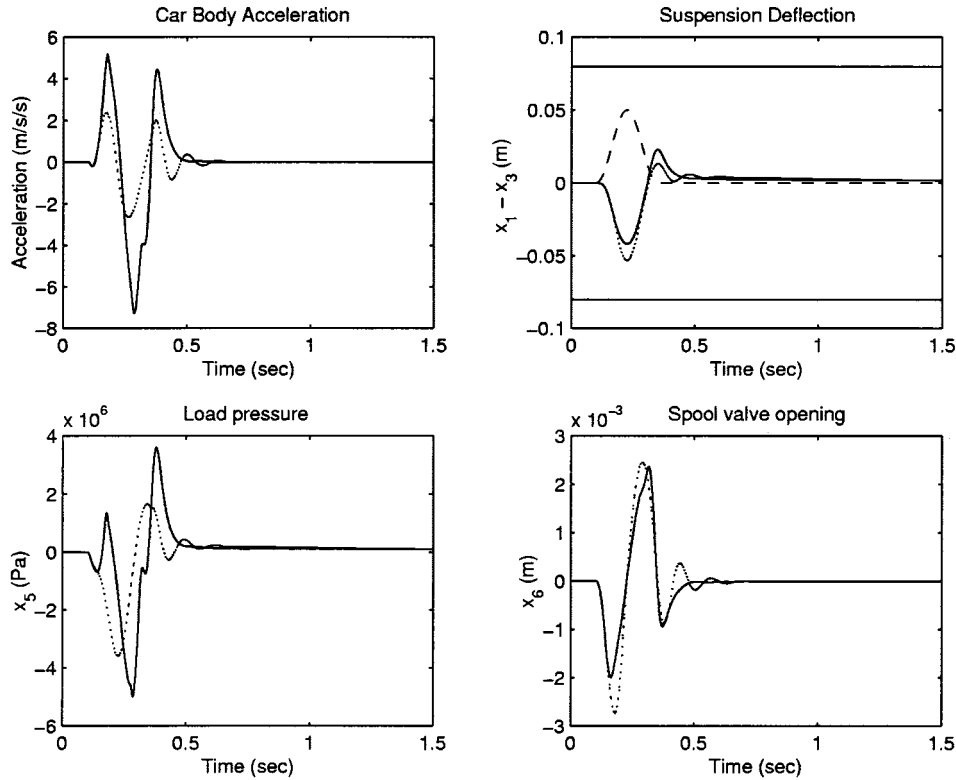

Fig. 6.   LPV controller responses to a 0.05-m bump, $\rho_r = 0.055$ (dotted), $\rho_r = 0.1$ (solid). The solid horizontal lines in the suspension deflection window are the deflection limits, while the dashed plot is the road disturbance.

The time responses of the nonlinear controller (LPV controller combined with the backstepping compensator) are shown in Figs. 6 and 7.

In the simulations, the LPV controller is implemented by setting the scheduling variable, ρ_{sd}, to be equal to the suspension deflection, i.e., $\rho_{sd}(t) = x_1(t) - x_3(t)$. The responses in Fig. 6 correspond to a small road bump of height 0.05 m (5 cm). The dotted responses correspond to the controller with ρ_r set equal to 0.055 (smooth road setting), while the solid responses correspond to $\rho_r = 0.1$ (rough road setting). Recall that when
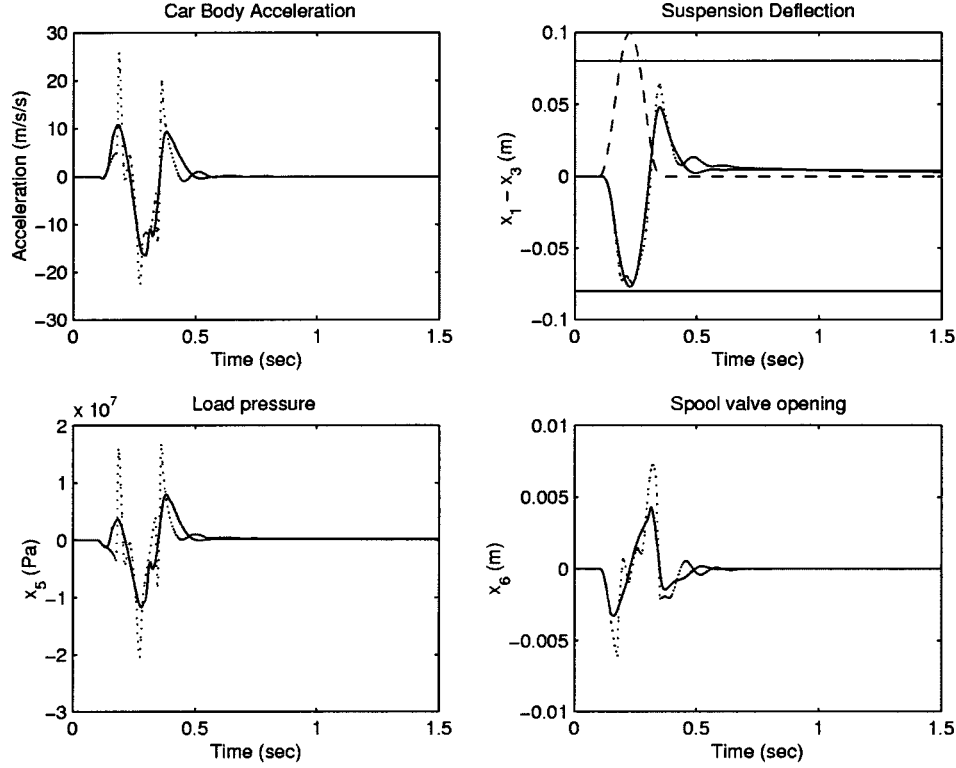
Fig. 7. LPV controller responses to a 0.1-m bump, $\rho_r = 0.055$ (dotted), $\rho_r = 0.1$ (solid). The solid horizontal lines in the suspension deflection window are the deflection limits, while the dashed plot is the road disturbance.

$\rho_r = 0.055$ the controller begins to shift focus from acceleration to deflection when the deflection exceeds 0.055 m. Since the size of the bump is only 0.05 m, this setting focuses exclusively on minimizing acceleration, and hence the vertical acceleration experienced by the car body is very small. On the other hand the controller with ρ_r set to 0.1 begins to shift focus from almost zero deflection. Smaller suspension deflection is generated and as a consequence the level of vertical acceleration is considerably higher. We conclude that, from the point of view of passenger comfort, over small bumps (smooth road sections) a road condition setting of $\rho_r = 0.055$ is preferable.

The responses in Fig. 7 correspond to a large road bump of height 0.1 m (10 cm). The dotted responses correspond to the controller with ρ_r set equal to 0.055 (smooth road setting), while the solid responses correspond to $\rho_r = 0.1$ (rough road setting). As can be seen from the dotted deflection responses, the controller with $\rho_r = 0.055$ begins to rapidly limit suspension deflection when the deflection exceeds 0.055 m. During this rapid stiffening a large vertical acceleration is transmitted to the car body. On the other hand the controller with $\rho_r = 0.1$ gradually limits deflection as it increases from zero to the deflection limit. Due to the fact that the stiffening is gradual, the level of vertical acceleration is significantly lower than achieved with the $\rho_r = 0.055$ setting. We conclude that, from the point of view of passenger comfort, over large bumps (rough road sections) a road condition setting of $\rho_r = 0.1$ is preferable.

Based on the above analysis, we conclude that superior passenger comfort over the whole range of road conditions is

achievable by automatically switching ρ_r between 0.055 and 0.1. Road adaptive switching of ρ_r is discussed next.

IV. ROAD ADAPTIVE SWITCHING

As seen in the previous section, a setting of $\rho_r = 0.055$ is preferable on smooth roads, while a setting of $\rho_r = 0.1$ is preferable on rough roads. Therefore, lower acceleration levels can be achieved over the range of road conditions, by adaptively switching ρ_r in response to the road conditions. In this section we discuss the use of the switching strategy presented in [14] to switch between controllers, based on current road conditions. Suspension deflection is used as a measure of road smoothness, and controllers are switched based on the following logic:

> Initialize ρ_r at 0.055.
> **I. Switching from 0.055 to 0.1:**
>   If $|x_1(t) - x_3(t)| > s_1$,
>   switch ρ_r to 0.1,
>   else, maintain ρ_r at 0.055.
> **II. Switching from 0.1 to 0.055:**
>   If $\max_{\tau \in [t - T_s, t]} |x_1(\tau) - x_3(\tau)| < s_2$,
>   switch ρ_r to 0.055,
>   else, maintain ρ_r at 0.1.

The first switching rule causes ρ_r to switch from the smooth road setting to the rough road setting when the road becomes rough. According to the second switching rule if ρ_r is currently at the rough road setting and the suspension deflection has remained below s_2 for at least T_s seconds, ρ_r is switched back to
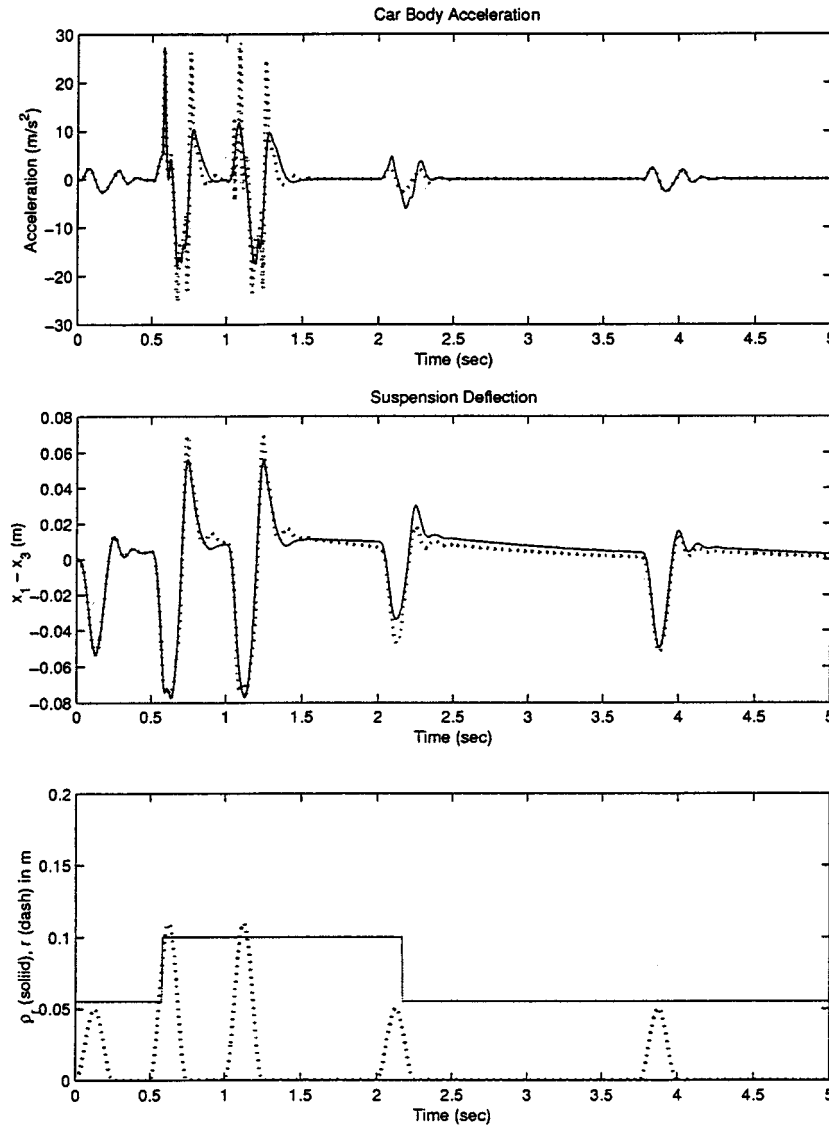
Fig. 8.   Road adaptive responses (solid). The dotted responses correspond to a constant ρ_r setting of 0.055. The dashed plot in the bottom window is the road profile.

0.055. Note that $s_1 \geq s_2$ due to the fact that suspension deflection under similar road conditions will be smaller for $\rho_r = 0.1$. We choose $s_1 = 0.065$ m, $s_2 = 0.05$ m and $T_s = 1$ second.

In order to avoid discontinuous jumps in the scheduling variable, $\rho_r(t)$ defined by the above switching rules is passed through a filter before it enters the LPV controller. We choose the filter to be $1/(0.08s + 1)$. In Fig. 8 the road adaptive response (solid) is compared with the response that corresponds to a constant ρ_r setting of 0.055 (dotted lines). During the first large bump a switching to $\rho_r = 0.1$ occurs, and hence during the remaining part of this bump, and during the second large bump lower car body accelerations are achieved. The controller switches back to $\rho_r = 0.055$ on the trailing edge of the second small bump. Both switched and $\rho_r = 0.055$ responses coincide over the third small bump. In Fig. 9 we compare the road adaptive responses (solid) with responses that correspond to a constant ρ_r setting of 0.1 (dotted lines). Over the larger bumps the acceleration responses are similar. Once again, due to the fact that the road adaptive controller switches to $\rho_r = 0.055$

under smooth road conditions, the acceleration levels over the first and last small bumps are lower than that achieved by the constant setting of $\rho_r = 0.1$.

We point out that since the LPV controller is defined for a ρ_r range of $[0, 0.1]$, a larger number of switching values could be used to further improve passenger comfort. This improvement however is achieved at the cost of a more complex switching logic.

V. CONCLUSION

In this paper we have presented a framework for designing road adaptive suspension controllers. Linear parameter-varying techniques were used in combination with nonlinear backstepping to achieve the desired nonlinear response of the vehicle suspension. The superiority of the road adaptive controllers has been demonstrated in nonlinear simulations. Since the present controller requires only ten controller values to be stored in memory, we expect it to be easily implementable as well.
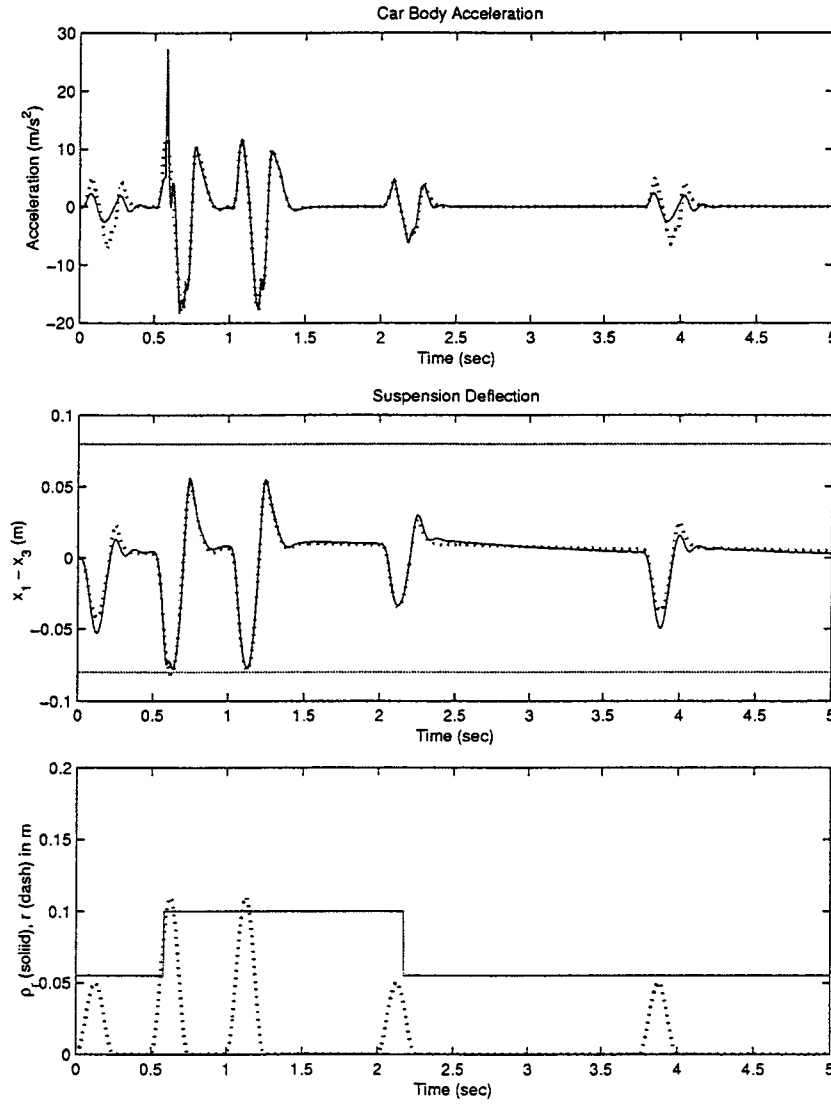
Fig. 9. Road adaptive responses (solid). The dotted responses correspond to a constant ρ_r setting of 0.1. The dashed plot in the bottom window is the road profile.

APPENDIX
LINEAR PARAMETER-VARYING CONTROL

In this appendix we provide a brief introduction to gain-scheduling based on linear parameter-varying (LPV) plant representations. For a compact subset $\mathcal{P} \subset \mathcal{R}^s$, the parameter variation set $\mathcal{F}_\mathcal{P}$ denotes the set of all piecewise continuous functions mapping $\mathcal{R}$ (time) into $\mathcal{P}$ with a finite number of discontinuities in any interval. From the point of view of control design it is assumed that the plant has the partitioned LPV representation

$$\begin{bmatrix} \dot{x}(t) \\ e(t) \\ y(t) \end{bmatrix} = \begin{bmatrix} A(\rho) & B_1(\rho) & B_2(\rho) \\ C_1(\rho) & D_{11}(\rho) & D_{12}(\rho) \\ C_2(\rho) & D_{21}(\rho) & D_{22}(\rho) \end{bmatrix} \begin{bmatrix} x(t) \\ d(t) \\ u(t) \end{bmatrix}. \quad (12)$$

Here $\rho \in \mathcal{F}_\mathcal{P}$, $y \in \mathcal{R}^{n_y}$ is the measurement, $u \in \mathcal{R}^{n_u}$ is the control input, $d \in \mathcal{R}^{n_d}$ is the exogenous disturbance, $e \in \mathcal{R}^{n_e}$ is the error output, and the state-space matrices are assumed to be continuous functions of the parameter ρ. It is assumed that the parameter $\rho(\cdot)$ can be measured in real time, and that the controller is of the form

$$\begin{bmatrix} \dot{x}_K(t) \\ u(t) \end{bmatrix} = \begin{bmatrix} A_K(\rho(t)) & B_K(\rho(t)) \\ C_K(\rho(t)) & D_K(\rho(t)) \end{bmatrix} \begin{bmatrix} x_K(t) \\ y(t) \end{bmatrix} \quad (13)$$

where $\rho \in \mathcal{F}_\mathcal{P}$.

The "quadratic LPV γ-performance problem" is to choose the parameter-varying controller matrices $A_K(\rho)$, $B_K(\rho)$, $C_K(\rho)$, $D_K(\rho)$ such that the resultant closed-loop system is quadratically stable and the induced $\mathcal{L}_2$ norm from d to e is $\leq \gamma$. The main synthesis result is that the existence of a controller that solves the quadratic LPV γ-performance problem can be expressed as the feasibility of a set of AMIs, which can be solved numerically. For more details on LPV synthesis results the reader is referred to [2], [3]. The parameter ρ is assumed to be available in real time, and hence it is possible to construct an LPV controller whose dynamics adjust according to variations in ρ, and maintain stability and performance along all parameter trajectories. This approach allows gain-scheduled controllers to be treated as a single entity, with the gain-scheduling achieved via the parameter-dependent controller.

REFERENCES

[1] A. Alleyne, P. D. Neuhaus, and J. K. Hedrick, "Application of nonlinear control theory to electronically controlled suspensions," *Vehicle System Dynamics*, vol. 22, pp. 309–320, 1993.

[2] G. Becker, "Quadratic stability and performance of linear parameter dependent systems," Ph.D. dissertation, Dept. Mech. Eng., Univ. California Berkeley, 1993.

[3] G. Becker and A. Packard, "Robust performance of linear parametrically varying systems using parametrically dependent linear dynamic feedback," *Syst. Contr. Lett.*, vol. 23, pp. 205–215, 1994.

[4] R. M. Chalasani, "Ride performance potential of active suspension systems—Part 1," in *ASME Monograph*, AMD vol. 80, DSC, vol 2.

[5] T. D. Gillespie, "Fundamentals of vehicle dynamics," Soc. Automotive Eng., 1990.

[6] J. K. Hedrick and T. Batsuen, "Invariant properties of automotive suspensions," in *Proc. Inst. Mech. Eng.*, vol. 204, 1990, pp. 21–27.

[7] D. Hrovat, "Optimal active suspension structures for quarter-car vehicle models," *Automatica*, vol. 26, pp. 845–860, 1990.

[8] ——, "Applications of optimal control to advanced automotive suspension design," *Trans. ASME, J. Dyn. Syst., Measurement, Contr.*, vol. 115, pp. 328–342, 1993.

[9] D. Karnopp, "Theoretical limitations in active vehicle suspensions," *Vehicle Syst. Dyn.*, vol. 15, pp. 41–54, 1986.

[10] K. Kawagoe and M. Iguchi, "Semi-active control and optimum preview control applications to vehicle suspensions," *JSAE Rev.*, pp. 24–31, 1985.

[11] M. Kristic, I. Kanellakopoulos, and P. Kokotovic, *Nonlinear and Adaptive Control Design*. New York: Wiley Interscience, 1995.

[12] J. Lin and I. Kanellakopoulos, "Adaptive nonlinear control in active suspensions," in *Preprints 13th World Congr. IFAC*, vol. F, San Francisco, CA, 1996, pp. 341–346.

[13] ——, "Nonlinear design of active suspensions," *Contr. Syst. Mag.*, vol. 17, pp. 45–59, 1997.

[14] ——, "Road adaptive nonlinear design of active suspensions," in *Proc. Amer. Contr. Conf.*, 1997, pp. 714–718.

[15] H. E. Merritt, *Hydraulic Control Systems*. New York: Wiley, 1967.

[16] R. Rajamani and J. K. Hedrick, "Adaptive observers for active automotive suspensions: Theory and experiment," *IEEE Trans. Contr. Syst. Technol.*, vol. 3, pp. 86–93, 1995.

[17] M. C. Smith, "Achievable dynamic response for automotive active suspensions," *Veh. Syst. Dyn.*, vol. 24, pp. 1–34, 1995.

[18] M. Sunwoo and K. C. Cheok, "An application of explicit self-tuning controller to vehicle active suspension systems," in *Proc. IEEE Conf. Decision Contr.*, 1990, pp. 2251–2255.

Ian Fialho was born in Bombay, India, on September 6, 1968. He received the B.Tech. degree in electrical and electronic engineering from the Regional Engineering College, Calicut, India, in 1989, the M. Tech. degree in electrical engineering from the Indian Institute of Technology, Bombay, in 1992, and the Ph.D. degree in control science and dynamical systems from the University of Minnesota, Minneapolis, in 1996.

From April 1992 to June 1996, he was a Research Assistant with the Department of Electrical Engineering at the University of Minnesota. In July 1996, he joined the Department of Aerospace Engineering at the University of Minnesota where he served as Assistant Professor and Associate Member of the graduate faculty until July 1998. He is currently with the Boeing Company, Houston, TX, where he works on microgravity vibration suppression control systems associated with the International Space Station. His research interests include performance and robustness issues in nonlinear control, sampled data control, multivariable robust control, and the application of these techniques to active vibration control, control of road vehicle dynamics, and the control of aircraft and missiles.

Dr. Fialho is currently an Associate Editor for the IEEE Control System Society Conference Editorial Board (CEB).

Gary J. Balas (S'89–M'89) received the B.S. and M.S. degrees in civil and electrical engineering from the University of California, Irvine, and the Ph.D. degree in aeronautics and astronautics from the California Institute of Technology, Pasadena, in 1990.

Since 1990, he has been a faculty member in the Department of Aerospace Engineering and Mechanics at the University of Minnesota, Minneapolis. From 1993 to 1995, he held a McKnight–Land Grant Professorship. Currently, he is an Associate Professor and Co-Director of the Control Science and Dynamical Systems Department at the University of Minnesota. He is a Co-Organizer and developer of the MUSYN Robust Control Short Course and the μ-Analysis and Synthesis Toolbox used with MATLAB and the President of MUSYN, Inc. His research interests include control of flexible structures, model validation and industrial applications of robust control methods.